Journal of Computational Mathematics
Vol.xx, No.x, 200x, 1–14.

http://www.global-sci.org/jcm
doi:10.4208/jcm.1910-m2019-0119

CAN A CUBIC SPLINE CURVE BE G^3*

Wujie Liu and Xin Li
School of Mathematical Science, University of Science and Technology of China, Hefei, Anhui, China
Email: lixustc@ustc.edu.cn

Abstract

This paper proposes a method to construct an G^3 cubic spline curve from any given open control polygon. For any two inner Bézier points on each edge of a control polygon, we can define each Bézier junction point such that the spline curve is G^2-continuous. Then by suitably choosing the inner Bézier points, we can construct a global G^3 spline curve. The curvature combs and curvature plots show the advantage of the G^3 cubic spline curve in contrast with the traditional C^2 cubic spline curve.

Mathematics subject classification: 65D07.
Key words: Cubic Spline, Geometric Continuity, G^3 Continuity.

1. Introduction

Curve modeling has a long history in computer graphics, which is widely used in drawing, sketching, data fitting, interpolation, as well as animation. The basic goal of curve modeling is to provide the algorithm to edit the shape of the curve with some certain geometric properties. In industrial or conceptual design, one important question is how to construct a fair freeform curve. Most CAD systems rely on some sort of curvature information to define a fair curve and the prevailing tools are curvature combs and curvature plots [30,31]. The most used representations in the industry design are cubic B-splines. However, the curvature plot or curvature comb has some non-smooth junctions because the spline curve is at most C^2-continuous, as shown in Figure 1.1. This leads a very nature question: can we increase the continuity of a cubic spline curve?

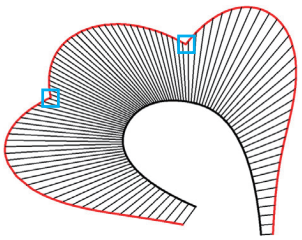

Fig. 1.1. The curvature comb of a cubic B-spline curve has some non-smooth junctions.

This paper gives a positive answer for this problem and proposes a method to construct a G^3 cubic spline curve for any given open control polygon. First, for the given control polygon, we

* Received May 8, 2019 / Revised version received October 15, 2019 / Accepted October 17, 2019 / Published online December 17, 2019 /

can select any two inner Bézier points on each edge and define the junction points to construct a global G^2 spline curve. And then, we can construct a global G^3 spline curve by solving the inner Bézier points. We prove that the solution always exists under a restriction on the control polygon. Same as the B-spline curve, the curve satisfies the convex hull property and can be modified by editing the control polygon. The curvature combs and curvature plots show the advantage of the G^3 cubic spline curve in contrast with the traditional C^2 cubic spline curve.

1.1. Related work

Among all the representations, Non-Uniform Rational B-Spline (NURBS) is the industry standard for the representation, design, and data exchange of geometric information processed by computers [2]. Many different models of splines have been introduced for various purpose. B-spline is introduced by Schoenberg [23] using divided difference which is not suitable for computing [3]. And then, C. de Boor [5] and M. Cox [6] discover the recurrence relations independently. The recurrence relation is used by Gordon and Riesenfeld [7] for efficient computing. The B-Spline can also be regarded as the basis functions of a linear spline space [4]. Beta-spline is introduced by Barsky [8] by replacing the derivatives with the tangent vector and curvature vector [9], which preserves the geometric smoothness of the curve and gives greater flexibility to control the shape [10, 11]. The definition of geometric continuity has been used by many other authors, such as Manning [12], Nielson [13], Barsky and DeRose [14] and Böhm [15]. Pythagorean hodograph (PH) spline curves are defined in [16], which provide rational offset curves and polynomial arc-length functions [17,18]. X-spline model is proposed in [19] to make user manipulations more intuitively. The other geometrical continuous spline curve constructions have been widely developed as well. Schaback [34] constructs a piecewise quadratic G^2 Bézier interpolatory curve by satisfying certain generalized convexity conditions. Yan et al. [33] construct almost everywhere curvature continuous piecewise quadratic curves, called κ–curves. Miura et al. [36] design log-aesthetic spline curves with G^2 continuity by solving the G^2 Hermite interpolation problem. Farin proposes the constructing of G^2 cubic spline with the given control polygon by using the Euclidean distances in [21,22]. The curvature continuous PH spline curves have been constructed from any control polygon in [32]. However, all of these constructions only involve G^2 continuity at most.

1.2. Organization

The rest of the paper is organized as follows. In Section 2, we recall some basic properties of B-spline and present the derivatives of a B-spline curve respecting the arc length. In Section 3, we derive the G^3 continuous condition and provide the algorithm to construct the G^3 cubic spline curves. We also prove that the solution always exists under a restriction on the control polygon. The examples of the present construction and traditional B-spline are shown in Section 4. Finally, Section 5 presents the conclusion and future work.

2. Cubic B-spline curves

Given a knot vector $U = \{u_{-2}, u_{-1}, u_0, \cdots, u_n, u_{n+1}, u_{n+2}\}$, $u_i \leq u_{i+1}$, $u_i < u_{i+4}$, and a set of control points P_i, $i = 0, \ldots, n$, a cubic B-spline curve is defined as

$$\mathbf{P}(u) = \sum_{i=0}^{n} B_i^3(u)\mathbf{P}_i, \tag{2.1}$$

where $B_i^3(u)$ is a cubic B-spline basis function defined by the following recursive relation,

$$B_i^0(u) = \begin{cases} 1, & \text{if} \quad u_{i-2} \le u < u_{i-1} \\ 0, & \text{otherwise} \end{cases}$$
$$B_i^d(u) = \frac{u - u_i}{u_{i+d} - u_i} B_i^{d-1}(u) + \frac{u_{i+d+1} - u}{u_{i+d+1} - u_{i+1}} B_{i+1}^{d-1}(u) \tag{2.2}$$

A B-spline curve can be extracted into a set of Bézier curves, i.e., each segment has Bézier control points $\{\mathbf{B}_{3i}, \mathbf{B}_{3i+1}, \mathbf{B}_{3i+2}, \mathbf{B}_{3(i+1)}\}_{i=0}^{n-3}$, by Böhm algorihtm [28] or blossom [?, 25, 26]. As shown in Figure 2.1(b), the points $\mathbf{B}_{3(i-1)+1}, \mathbf{B}_{3(i-1)+2}$ are called inner Bézier points, and the points $\mathbf{B}_{3i}$ are junction points. Let knot interval $d_i = u_{i+1} - u_i$, then we have

$$\begin{cases} |\overrightarrow{\mathbf{P}_i\mathbf{B}_{3i-2}}| : |\overrightarrow{\mathbf{B}_{3i-2}\mathbf{B}_{3i-1}}| : |\overrightarrow{\mathbf{B}_{3i-1}\mathbf{P}_{i+1}}| = d_{i-1} : d_i : d_{i+1}, \\ |\overrightarrow{\mathbf{B}_{3i-1}\mathbf{B}_{3i}}| : |\overrightarrow{\mathbf{B}_{3i}\mathbf{B}_{3i+1}}| = d_i : d_{i+1}. \end{cases}$$

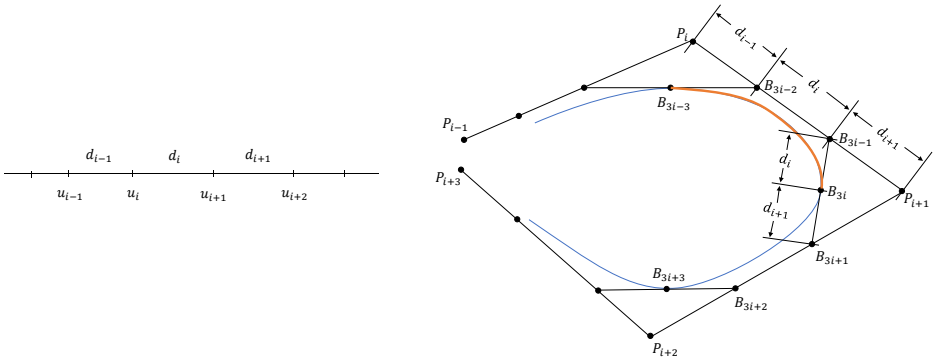

(a) Knot intervals (b) Bézier control points

Fig. 2.1. Extract the Bézier control points for each segment of a cubic spline curve.

2.1. Derivative of a B-spline curve

Let $\mathbf{P}(u)$ be a regular planar curve, then the derivatives of $\mathbf{P}(u)$ with respecting to arc length s is

$$\frac{\mathrm{d}\mathbf{P}}{\mathrm{d}s} = \mathbf{t}(s) = \frac{\mathrm{d}\mathbf{P}}{\mathrm{d}u} / (\frac{\mathrm{d}s}{\mathrm{d}u}) = \frac{\mathbf{P}'}{|\mathbf{P}'|}, \tag{2.3}$$

where primes denote differentiation respecting to u and $\mathbf{t}(s)$ represents the tangent vector of the curve $\mathbf{P}$.

According to the equality $\mathbf{P} \cdot \mathbf{P} = |\mathbf{P}|^2$, we can obtain $\mathbf{P} \cdot \mathbf{P}' = |\mathbf{P}| \, (\mathrm{d}|\mathbf{P}|/\mathrm{d}u)$ by differentiation. Using this equality, we can get the second derivative,

$$\begin{aligned} \frac{\mathrm{d}^2\mathbf{P}}{\mathrm{d}s^2} &= \kappa(s)\mathbf{n}(s) = \frac{\mathrm{d}}{\mathrm{d}s}(\frac{\mathrm{d}\mathbf{P}}{\mathrm{d}s}) = \frac{\mathrm{d}}{\mathrm{d}u}(\frac{\mathbf{P}'}{|\mathbf{P}'|})/s' \\ &= \frac{1}{|\mathbf{P}'|}(\frac{\mathbf{P}''}{|\mathbf{P}'|} - \frac{\mathbf{P}'}{|\mathbf{P}'|^2} \cdot \frac{\mathrm{d}|\mathbf{P}'|}{\mathrm{d}u}) \\ &= \frac{\mathbf{P}''}{\mathbf{P}' \cdot \mathbf{P}'} - \frac{\mathbf{P}' \cdot \mathbf{P}''}{(\mathbf{P}' \cdot \mathbf{P}')^2}\mathbf{P}' = \frac{\mathbf{P}' \times (\mathbf{P}'' \times \mathbf{P}')}{(\mathbf{P}' \cdot \mathbf{P}')^2}, \end{aligned} \tag{2.4}$$

where $\mathbf{n}(s)$ is the normal vector and $\kappa(s)$ is the curvature. The equality 2.4 uses the vector triple product $\mathbf{a}\times(\mathbf{b}\times\mathbf{c})=(\mathbf{a}\cdot\mathbf{c})\mathbf{b}-(\mathbf{a}\cdot\mathbf{b})\mathbf{c}$.

The third derivative can be defined as

$$\begin{aligned}\frac{\mathrm{d}^3\mathbf{P}}{\mathrm{d}s^3}&=\kappa'(s)\mathbf{n}(s)-\kappa^2(s)\mathbf{t}(s)=\frac{1}{|\mathbf{P}'|}\frac{\mathrm{d}}{\mathrm{d}u}\Big(\frac{\mathbf{P}'\times(\mathbf{P}''\times\mathbf{P}')}{(\mathbf{P}'\cdot\mathbf{P}')^2}\Big)\\&=\frac{\mathbf{P}''\times(\mathbf{P}''\times\mathbf{P}')+\mathbf{P}'\times(\mathbf{P}'''\times\mathbf{P}')}{|\mathbf{P}'|\cdot(\mathbf{P}'\cdot\mathbf{P}')^2}-\frac{4(\mathbf{P}''\cdot\mathbf{P}')\mathbf{P}'\times(\mathbf{P}''\times\mathbf{P}')}{|\mathbf{P}'|\cdot(\mathbf{P}'\cdot\mathbf{P}')^3}.\end{aligned}\tag{2.5}$$

For two planar vectors $\mathbf{a},\mathbf{b}$ and a nonzero vector $\mathbf{c}$, there exists the below equivalent relation

$$\mathbf{a}=\mathbf{b}\Leftrightarrow\begin{cases}\mathbf{a}\times\mathbf{c}=\mathbf{b}\times\mathbf{c}\\ \mathbf{a}\cdot\mathbf{c}=\mathbf{b}\cdot\mathbf{c}.\end{cases}\tag{2.6}$$

Using the vector calculus, we can obtain the dot and cross product of first derivative and third derivative by the above equalities.

$$\frac{\mathrm{d}\mathbf{P}}{\mathrm{d}s}\cdot\frac{\mathrm{d}^3\mathbf{P}}{\mathrm{d}s^3}=\frac{(\mathbf{P}'\cdot\mathbf{P}'')^2-(\mathbf{P}'\cdot\mathbf{P}')(\mathbf{P}''\cdot\mathbf{P}'')}{(\mathbf{P}'\cdot\mathbf{P}')^3}=-\frac{|\mathbf{P}'\times\mathbf{P}''|^2}{(\mathbf{P}'\cdot\mathbf{P}')^3}\tag{2.7}$$

$$\frac{\mathrm{d}\mathbf{P}}{\mathrm{d}s}\times\frac{\mathrm{d}^3\mathbf{P}}{\mathrm{d}s^3}=\kappa'(s)\mathbf{t}(s)\times\mathbf{n}(s)=-3\frac{(\mathbf{P}'\cdot\mathbf{P}'')(\mathbf{P}'\times\mathbf{P}'')}{(\mathbf{P}'\cdot\mathbf{P}')^3}+\frac{\mathbf{P}'\times\mathbf{P}'''}{(\mathbf{P}'\cdot\mathbf{P}')^2}.\tag{2.8}$$

We will take the following definition for the consideration of geometric continuity.

Definition 2.1. *Two curves are n-order geometric continuity (G^n) at a common point, if and only if they are C^n continuous with respect to their respective arc length at this point.*

3. Framework to construct G^3 cubic spline curves

In this section, we construct the G^3 cubic spline curves from any given open control polygon by solving a non-linear system. We prove that the solution of the system always exists under a restriction on the control polygon.

3.1. G^2 spline curve construction

Given a set of ordered control points $\mathbf{P}_0,\mathbf{P}_1,\cdots,\mathbf{P}_n$, a set of knot intervals d_i, $i=-1,0,\ldots,n$, we can create a global G^2 spline curves by the following simple construction. First, we associate each interior edge $\mathbf{P}_i\mathbf{P}_{i+1}$ with a parameter $\lambda_i\in(0,1), i=0,1,\cdots,n-1$. Then we can extract the two inner Bézier control points according to the following equations,

$$|\overrightarrow{\mathbf{B}_{3(i-1)+1}\mathbf{B}_{3(i-1)+2}}|=\lambda_i|\overrightarrow{\mathbf{P}_i\mathbf{P}_{i+1}}|,\tag{3.1}$$

$$|\overrightarrow{\mathbf{P}_i\mathbf{B}_{3(i-1)+1}}|=\frac{d_{i-1}}{d_{i-1}+d_{i+1}}(1-\lambda_i)|\overrightarrow{\mathbf{P}_i\mathbf{P}_{i+1}}|,\tag{3.2}$$

$$|\overrightarrow{\mathbf{B}_{3(i-1)+2}\mathbf{P}_{i+1}}|=\frac{d_{i+1}}{d_{i-1}+d_{i+1}}(1-\lambda_i)|\overrightarrow{\mathbf{P}_i\mathbf{P}_{i+1}}|.\tag{3.3}$$

The junction point $\mathbf{B}_{3i}(i=0,1,\cdots,n-2)$ is determined by G^2 condition,

$$\mathbf{B}_{3i}=\frac{\delta_i\mathbf{B}_{3i-1}+\mathbf{B}_{3i+1}}{1+\delta_i},\tag{3.4}$$

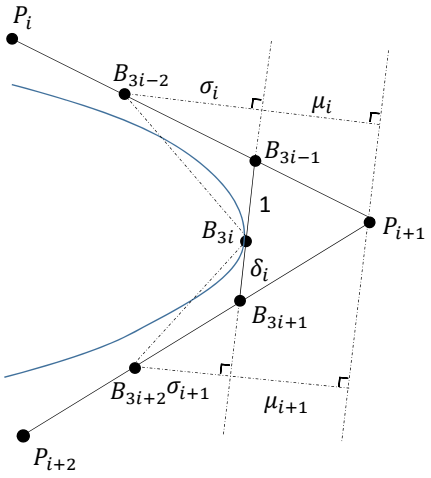

Fig. 3.1. The determination of Bézier junction point with G^2 conditon

where

$$\delta_i^2 := \left(\frac{|B_{3i+1} - B_{3i}|}{|B_{3i} - B_{3i-1}|}\right)^2 = \frac{d_{i+1}(d_i + d_{i+2})}{d_i(d_{i-1} + d_{i+1})} \cdot \frac{\lambda_{i+1}(1-\lambda_i)}{\lambda_i(1-\lambda_{i+1})}.$$

Remark 3.1. If $\lambda_i = \frac{d_i}{d_{i-1}+d_i+d_{i+1}}$, the above construction will produce the cubic B-spline curve. And if $d_{-1} = d_0 = d_{n-1} = d_n = 0$, the final spline curve will interpolate the two end points P_0 and P_n.

Remark 3.2. If $\mathbf{P}_0 = \mathbf{P}_n$ and the spline curve corresponds a close curve, we can consider the indices for the control points and knot intervals in terms of the module of n, and then we can construct a global G^2 curve in the similar procedure.

If the control polygon is open, then the spline curve can be extracted into $n-2$ Bézier segments. And for any $\lambda_i \in (0,1)$, we can construct a G^2 spline curve. So the basic idea of the paper is to optimize the parameters λ_i such that the final spline curve has higher order of continuity.

3.2. G^3 constraints

For the purpose of considering the higher continuity at the junction point $\mathbf{B}_{3i}$, we reparameterize the spline of $\mathbf{P}(u)$ near the point $\mathbf{B}_{3i}$. Denote the left Bézier segment by $\mathbf{L}(\alpha)$ and right by $\mathbf{R}(\beta)$, as shown in the Figure 3.2.

Concretely, $\mathbf{L}(\alpha)$ is the Bézier segment with control points $\mathbf{B}_{3i-3}, \mathbf{B}_{3i-2}, \mathbf{B}_{3i-1}, \mathbf{B}_{3i}$ and $\mathbf{R}(\beta)$ is the Bézier segment with control points $\mathbf{B}_{3i}, \mathbf{B}_{3i+1}, \mathbf{B}_{3i+2}, \mathbf{B}_{3i+3}$, i.e.,

$$\mathbf{L}(\alpha) = \sum_{j=0}^{3} \mathbf{B}_{3(i-1)+j} \binom{j}{3} \alpha^j (1-\alpha)^{3-j},\ 0 \le \alpha \le 1;$$

$$\mathbf{R}(\beta) = \sum_{j=0}^{3} \mathbf{B}_{3i+j} \binom{j}{3} \beta^j (1-\beta)^{3-j},\ 0 \le \beta \le 1.$$

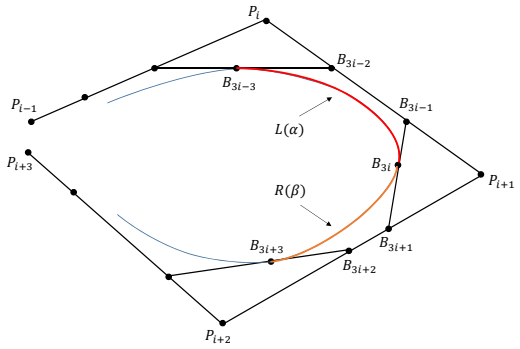

Fig. 3.2. Re-parametrization

By the differential calculus, we can obtain the below expressions.

$$\begin{aligned}
&\mathbf{L}'(1) = 3(\mathbf{B}_{3i} - \mathbf{B}_{3i-1}) = 3\Delta\mathbf{B}_{3i-1},\\
&\mathbf{L}''(1) = 6(\Delta\mathbf{B}_{3i-1} - \Delta\mathbf{B}_{3i-2}),\\
&\mathbf{L}'''(1) = 6(\Delta\mathbf{B}_{3i-1} - 2\Delta\mathbf{B}_{3i-2} + \Delta\mathbf{B}_{3i-3}),\\
&\mathbf{R}'(0) = 3(\mathbf{B}_{3i+1} - \mathbf{B}_{3i}) = 3\Delta\mathbf{B}_{3i},\\
&\mathbf{R}''(0) = 6(\Delta\mathbf{B}_{3i+1} - \Delta\mathbf{B}_{3i}),\\
&\mathbf{R}'''(0) = 6(\Delta\mathbf{B}_{3i+2} - 2\Delta\mathbf{B}_{3i+1} + \Delta\mathbf{B}_{3i}).
\end{aligned}$$

Due to $\frac{\mathrm{d}\mathbf{P}}{\mathrm{d}s}\cdot\frac{\mathrm{d}^3\mathbf{P}}{\mathrm{d}s^3} = -\kappa^2(s) = -\frac{\mathrm{d}^2\mathbf{P}}{\mathrm{d}s^2}\cdot\frac{\mathrm{d}^2\mathbf{P}}{\mathrm{d}s^2}$, we only need to consider the equation 2.7 according to the equivalent relation 2.6. The G^3 continuity condition of the curve $\mathbf{P}(u)$ at the point $\mathbf{B}_{3i}$ is deduced to

$$\left(-3\frac{(\mathbf{L}'\cdot\mathbf{L}'')(\mathbf{L}'\times\mathbf{L}'')}{(\mathbf{L}'\cdot\mathbf{L}')^3} + \frac{\mathbf{L}'\times\mathbf{L}'''}{(\mathbf{L}'\cdot\mathbf{L}')^2}\right)(1) = \left(-3\frac{(\mathbf{R}'\cdot\mathbf{R}'')(\mathbf{R}'\times\mathbf{R}'')}{(\mathbf{R}'\cdot\mathbf{R}')^3} + \frac{\mathbf{R}'\times\mathbf{R}'''}{(\mathbf{R}'\cdot\mathbf{R}')^2}\right)(0). \tag{3.5}$$

Remark 3.3. The cross product of two planar vectors is a vector perpendicular to the plane, so we only need to consider the norm of the product vector and the direction of the product vector is inward or outward of the plane.

3.3. Construct a G^3 cubic spline curve

From the equations 3.1 and 3.4, the Bézier points $\mathbf{B}_{3i-3}, \mathbf{B}_{3i-2}, \cdots, \mathbf{B}_{3i+3}$ can be represented by the control points $\mathbf{P}_{i-1}, \mathbf{P}_i, \mathbf{P}_{i+1}, \mathbf{P}_{i+2}, \mathbf{P}_{i+3}$ and the parameters $\lambda_{i-1}, \lambda_i, \lambda_{i+1}, \lambda_{i+2}$ such that the final curve is G^3 condition at the Bézier junction point $\mathbf{B}_{3i}$ $(i = 1, \cdots, n-3)$. The constraint is an equation involves unknowns $\lambda_{i-1}, \lambda_i, \lambda_{i+1}, \lambda_{i+2}$, which is denoted as

$$f_i(\mathbf{P_{i-1}}, \mathbf{P_i}, \mathbf{P_{i+1}}, \mathbf{P_{i+2}}, \mathbf{P_{i+3}}; \lambda_{i-1}, \lambda_i, \lambda_{i+1}, \lambda_{i+2}) = 0. \tag{3.6}$$

For an open curve, there are $n-3$ constraints and we have n unknowns. So we fix the λ_0 and λ_{n-1} and try to solved the other λ_i such that the constructed G^2 cubic spline curve is G^3 at every Bézier junction point $\mathbf{B}_{3i}, i = 1, 2, \cdots, n-3$. Finally, the G^3 constraints are formalized in this nonlinear system with unknowns λ_is, which can be solved by damped least-squares method. The nonlinear system is solved by the function *fsolve* in MATLAB 2018b, which is called by a project of visual studio 2017. The programming is implemented in C++ under the Windows 7 system, based on the Qt class with interactive design. For each parameter λ_i, we

assign a default value $\lambda_i = \frac{d_i}{d_{i-1}+d_i+d_{i+1}}, i = 0, 1, \cdots, n-1$. The algorithm can be formulated as following.

Algorithm 3.1. Framework of constructing G^3 spline curve

Input: The set of control points $\{\mathbf{P}_0, \mathbf{P}_1, \cdots, \mathbf{P}_n\}$;
Output: The control points $\mathbf{B}_i$ of $(n-2)$ Bézier segments;
1: Assign every polygon leg $\mathbf{P}_i\mathbf{P}_{i+1}$ a parameter $\lambda_i \in (0,1)$ and set a default value $\lambda_i = \frac{d_i}{d_{i-1}+d_i+d_{i+1}}, i = 0, 1, \cdots, n-1$.
2: Formulate the nonlinear system 3.6 according to the expressions 3.1, 3.4 and equation 3.5;
3: Solve the system 3.6 by damped least-squares method according to $\lambda_i, i = 1, \ldots, n-2$ and get the solution $\overline{\Lambda} = \{\overline{\lambda_1}, \cdots, \overline{\lambda_{n-2}}\}$;
4: Compute the interior Bézier points $\mathbf{B}_{3i+1}, \mathbf{B}_{3i+2}$ with $\overline{\Lambda}$ by 3.1;
5: Compute the junction point $\mathbf{B}_{3i}$ with $\overline{\Lambda}$ by 3.4;
return the control points of Bézier segments $\{\mathbf{B}_{3i}, \mathbf{B}_{3i+1}, \mathbf{B}_{3i+2}, \mathbf{B}_{3i+3}\}$, $i = 0, 1, \cdots, n-3$.

Remark 3.4. In the non-linear solver, the initial value is extremely important. In our implementation, we always set the initial value $\lambda_i = \frac{d_i}{d_{i-1}+d_i+d_{i+1}}, i = 0, 1, \cdots, n-1$. And in all the testing examples of interactive editing system, it always gives the solution for the initial values.

3.4. The Existence of the parameters λ_i

As we known, it is a difficult task to solve a non-linear system. And in general it may have no solution. But for our non-linear system, we prove that the solution always exists under a restriction on the control polygon, as shown in the theorem 3.1.

Theorem 3.1. *Given a open control polygon with control points $\mathbf{P}_0, \mathbf{P}_1, \cdots, \mathbf{P}_n, n \geq 3$, suppose for any $i = 0, 1, \cdots, n-1$, $\Delta\mathbf{P}_i \times \Delta\mathbf{P}_{i+1} \neq 0$, and for any $i = 1, \cdots, n-2$, $\tau_i > 0$ or $\tau_{i+1} > 0$, where $\tau_i = (\Delta\mathbf{P}_{i-1} \times \Delta\mathbf{P}_i) \cdot (\Delta\mathbf{P}_i \times \Delta\mathbf{P}_{i+1})$. Then the G^3 continuity nonlinear system 3.6 has a solution $\overline{\Lambda} = \{\overline{\lambda_1}, \overline{\lambda_2}, \cdots, \overline{\lambda_{n-2}}\}$, $0 < \overline{\lambda_i} < 1, i = 1, \cdots, n-2$.*

Proof. We prove the theorem by induction on the number of Bézier segments $l = n-2\,(n \geq 3)$. If $n = 3$, the spline curve only has one Bézier segment without any constraint. Thus the lemma is right obviously for any shape of control polygon and any $\lambda_0, \lambda_1, \lambda_2$. Assume the theorem is correct for $n < m$ and now we consider $n = m$. Suppose the control polygon is $\mathbf{P}_i$, $i = 0, \ldots, m$, then for any $1 < i < m$, and any λ_0, λ_i, λ_{i+1}, λ_{m-1}, according to the assumption, there exist $\lambda_1, \lambda_2, \cdots, \lambda_{i-1}$ such that $\mathbf{P}_0, \mathbf{P}_1, \ldots, \mathbf{P}_i$, $\mathbf{B}_{3i-1}, \mathbf{B}_{3i}$ can define a G^3 spline curve $\mathbf{C}_l$ and there exist $\lambda_{i+2}, \lambda_{i+3}, \cdots, \lambda_{m-2}$ such that $\mathbf{B}_{3i}, \mathbf{B}_{3i+1}$, $\mathbf{P}_{i+2}, \mathbf{P}_{i+3}, \ldots, \mathbf{P}_n$ can define a G^3 spline curve $\mathbf{C}_r$. Thus, we only need to prove that there exists appropriate $\lambda_i, \lambda_{i+1}, 0 < \lambda_i, \lambda_{i+1} < 1$ such that the spline curve is G^3 at $\mathbf{B}_{3i}$, where

$$\mathbf{B}_{3i} = \frac{1}{1+\delta_i}(\delta_i \mathbf{B}_{3i-1} + \mathbf{B}_{3i+1})$$

and

$$\delta_i = \left(\frac{d_{i+1}(d_i + d_{i+2})}{d_i(d_{i-1} + d_{i+1})} \cdot \frac{\lambda_{i+1}(1-\lambda_i)}{\lambda_i(1-\lambda_{i+1})}\right)^{\frac{1}{2}}.$$

As shown in the Figure 3.3, for the point $\mathbf{P}_{i+1}$, there are four different possible situations to be considered. The first is that $\tau_i > 0$ and $\tau_{i+1} > 0$, the second one is that $\tau_i < 0$ and $\tau_{i+1} > 0$, the third one is that $\tau_i > 0$ and $\tau_{i+1} < 0$, and the fourth is $\tau_i < 0$ and $\tau_{i+1} < 0$ which is not allowed in the present proof.

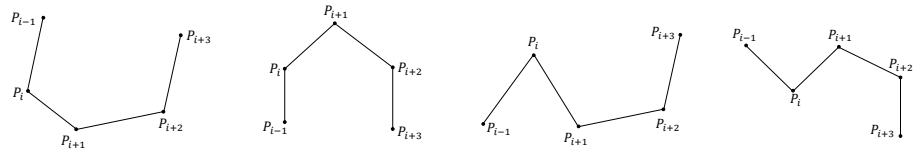

(a) $\tau_i > 0$ and $\tau_{i+1} > 0$ (b) $\tau_i < 0$ and $\tau_{i+1} > 0$

(c) $\tau_i > 0$ and $\tau_{i+1} < 0$ (d) $\tau_i < 0$ and $\tau_{i+1} < 0$

Fig. 3.3. Four possible situations for point $\mathbf{P}_{i+1}$, where the fourth one is not allowed in the proof of the theorem.

The proof of the three situations are analogous. Specifically, we fix λ_i or λ_{i+1} for the first situation and fix λ_i for the second situation while fix λ_{i+1} for the third situation. We present the detail proof for the first situation. The discussion of other situation is similar. By fixing the λ_i, let λ_{i+1} change from 0 to 1, δ_i will change from 0 to ∞. So, $\mathbf{B}_{3i+1}$ and $\mathbf{B}_{3i+2}$ will change from the central region of the polygon edge $\mathbf{P}_{i+1}\mathbf{P}_{i+2}$ to $\mathbf{P}_{i+1}$ and $\mathbf{P}_{i+2}$ respectively. And $\mathbf{B}_{3i}$ will change from $\mathbf{B}_{3i+1}$ to $\mathbf{B}_{3i-1}$.

Let E_l = the left side of Eq. (3.5) and E_r = the right side of Eq. (3.5), i.e.,

$$E_l = \frac{4\big(\Delta\mathbf{B}_{3i-1}\cdot(2\Delta\mathbf{B}_{3i-1}-3\Delta\mathbf{B}_{3i-2})\big)(\Delta\mathbf{B}_{3i-1}\times\Delta\mathbf{B}_{3i-2})}{9(\Delta\mathbf{B}_{3i-1}\cdot\Delta\mathbf{B}_{3i-1})^3}+\frac{2\Delta\mathbf{B}_{3i-1}\times\Delta\mathbf{B}_{3i-3}}{9(\Delta\mathbf{B}_{3i-1}\cdot\Delta\mathbf{B}_{3i-1})^2},$$
$$E_r = \frac{4\big(\Delta\mathbf{B}_{3i}\cdot(2\Delta\mathbf{B}_{3i}-3\Delta\mathbf{B}_{3i+1})\big)(\Delta\mathbf{B}_{3i}\times\Delta\mathbf{B}_{3i+1})}{9(\Delta\mathbf{B}_{3i}\cdot\Delta\mathbf{B}_{3i})^3}+\frac{2\Delta\mathbf{B}_{3i}\times\Delta\mathbf{B}_{3i+2}}{9(\Delta\mathbf{B}_{3i}\cdot\Delta\mathbf{B}_{3i})^2}.$$

Then, we have

$$\lim_{\lambda_{i+1}\to 0} E_l = c_1$$

which is a constant. On the other hand, $\lim\limits_{\lambda_{i+1}\to 0} E_r = \frac{0}{0}$ is indeterminate form, but we can analyze the order of the indeterminate to know it diverges to $+\infty$.

We can represent E_l, E_r with $\mathbf{P}_i$ and λ_i by the expression 3.1 and 3.4. Then we separate the λ_i part from E_l and E_r, and denote the other part by below symbols for ease of notations. We just show the detail expression of E_r, cause the similar consideration can be done with E_l.

Let

$$\varphi_i = \sqrt{d_{i+1}(d_i + d_{i+2})}, \tag{3.7}$$
$$\psi_i = \sqrt{d_i(d_{i-1} + d_{i+1})}, \tag{3.8}$$
$$\omega_i = \varphi_i\sqrt{\lambda_{i+1}(1-\lambda_i)} + \psi_i\sqrt{\lambda_i(1-\lambda_{i+1})}; \tag{3.9}$$
$$\mathbf{R}_i = \frac{d_{i+1}(\lambda_i - 1)}{d_{i-1}+d_{i+1}}\mathbf{P}_i + \left(\frac{d_i\lambda_{i+1}+d_{i+2}}{d_i+d_{i+2}} - \frac{d_{i-1}+d_{i+1}\lambda_i}{d_{i-1}+d_{i+1}}\right)\mathbf{P}_{i+1} + \frac{d_i(1-\lambda_{i+1})}{d_i+d_{i+2}}\mathbf{P}_{i+2}, \tag{3.10}$$

and $\mathbf{Q}_i = \Delta\mathbf{P}_i := \mathbf{P}_{i+1} - \mathbf{P}_i$, we have

$$\begin{aligned}E_r =&\Big(\frac{4\varphi_i^2\lambda_{i+1}^2(1-\lambda_i)}{\omega_i^2}\mathbf{R}_i\cdot\big(\frac{2\varphi_i\sqrt{\lambda_{i+1}(1-\lambda_i)}}{\omega_i}\mathbf{R}_i - 3\lambda_{i+1}\mathbf{Q}_{i+1}\big)(\mathbf{R}_i\times\mathbf{Q}_{i+1})\\ &+\frac{\varphi_i^2\lambda_{i+1}(1-\lambda_i)}{\omega_i^2}\mathbf{R}_i\cdot\mathbf{R}_i\big(\frac{2\varphi_i\sqrt{\lambda_{i+1}(1-\lambda_i)}}{\omega_i}\mathbf{R}_i\times\frac{\psi_{i+1}\sqrt{\lambda_{i+1}(1-\lambda_{i+2})}}{\omega_{i+1}}\mathbf{R}_{i+1}\big)\Big)\\ &\Big/\Big(9\big(\frac{\varphi_i^2\lambda_i(1-\lambda_i)}{\omega_i^2}\mathbf{R}_i\cdot\mathbf{R}_i\big)^3\Big).\end{aligned}$$

In order to analysis the order of the expression, we organize the numerator and denominator of the expression to

$$\begin{aligned}E_r =&\omega_i^3\Big(4\omega_{i+1}\varphi_i^2\lambda_{i+1}^{\frac{5}{2}}(1-\lambda_i)\mathbf{R}_i\cdot\big(2\varphi_i\sqrt{1-\lambda_i}\mathbf{R}_i - 3\omega_i\sqrt{\lambda_{i+1}}\mathbf{Q}_{i+1}\big)(\mathbf{R}_i\times\mathbf{Q}_{i+1})\\ &+2\varphi_i^3\psi_{i+1}\lambda_{i+1}^2(1-\lambda_i)^{\frac{3}{2}}(1-\lambda_{i+2})^{\frac{1}{2}}\mathbf{R}_i\cdot\mathbf{R}_i(\mathbf{R}_i\times\mathbf{R}_{i+1})\Big)\\ &\Big/\Big(9\omega_{i+1}\varphi_i^6\lambda_{i+1}^3(1-\lambda_i)^3(\mathbf{R}_i\cdot\mathbf{R}_i)^3\Big).\end{aligned}\tag{3.11}$$

From the above analysis of the order of E_l, E_r about λ_i, we have the asymptotic relation

$$\begin{aligned}E_l &\sim \frac{O\big(\lambda_i^{\frac{5}{2}}(1-\lambda_{i+1})\big)+O\big(\lambda_i^2(1-\lambda_{i+1})^{\frac{3}{2}}(1-\lambda_{i-1})^{\frac{1}{2}}\big)}{O\big(\lambda_i^3(1-\lambda_{i+1})^3\big)},\\ E_r &\sim \frac{O\big(\lambda_{i+1}^{\frac{5}{2}}(1-\lambda_i)\big)+O\big(\lambda_{i+1}^2(1-\lambda_i)^{\frac{3}{2}}(1-\lambda_{i+2})^{\frac{1}{2}}\big)}{O\big(\lambda_{i+1}^3(1-\lambda_i)^3\big)}.\end{aligned}$$

When we eliminate λ_{i+1}^2 from denominator and numerator of E_r, we can know the denominator tends to 0 but the numerator not. Consequently $\lim\limits_{\lambda_{i+1}\to 0} E_r = \pm\infty$, and the sign depend on the numerator. More concretely, the sign rely on the sign of numerator's second term $\Delta\mathbf{B}_{3i}\times\Delta\mathbf{B}_{3i+2}$ since the first term tends to 0. If we take the outward direction of the paper as sign +, we know the sign of the $\Delta\mathbf{B}_{3i}\times\Delta\mathbf{B}_{3i+2}$ is positive according to the right hand rule of vector cross product. We then have

$$\lim_{\lambda_{i+1}\to 0} E_r = +\infty.$$

When $\lambda_{i+1}\to 1$, we have

$$\lim_{\lambda_{i+1}\to 1} E_r = c_2$$

which is another constant. And $\lim\limits_{\lambda_{i+1}\to 1} E_l = \frac{0}{0}$ is indeterminate form. We can analysis the order of the indeterminate to know it is also $+\infty$ with the similar consideration of last paragraph. Because the denominator tends to 0 but the numerator not. The sign depends on the first term of numerator cause the second term tends to 0. While λ_{i+1} tends to 1, $\mathbf{B}_{3i}$ tends to $\mathbf{B}_{3i-1}$ and $\mathbf{B}_{3i+1}$ tends to $\mathbf{P}_{i+1}$. So, $2\Delta\mathbf{B}_{3i-1}\cdot\Delta\mathbf{B}_{3i-1} - 3\Delta\mathbf{B}_{3i-1}\cdot\Delta\mathbf{B}_{3i-2}$ is a negative number and $\Delta\mathbf{B}_{3i-1}\times\Delta\mathbf{B}_{3i-2}$ is also a negative number(actually a vector perpendicular to the paper with inward direction). Therefore,

$$\lim_{\lambda_{i+1}\to 1} E_l = +\infty.$$

Consequently, we have

$$\lim_{\lambda_{i+1}\to 0} E_l - E_r = -\infty, \quad \lim_{\lambda_{i+1}\to 1} E_l - E_r = +\infty.\tag{3.12}$$

According to the zero theorem, there must be exist a $\overline{\lambda_{i+1}}$ such that $E_l(\overline{\lambda_{i+1}}) = E_r(\overline{\lambda_{i+1}})$. The proof is complete.

Remark 3.5. Although the proof cannot be applied for the case of $\tau_i < 0$ and $\tau_{i+1} < 0$, but all our numerical experiment show that the solution always exists. So a better proof needs more consideration which is left as a further work.

4. Numerical Results

In this section, we list some examples to compare the new G^3 spline curve with the traditional cubic B-spline curves. In each example, the two representations have the same control polygon and knot intervals. We can also see that in all the examples, the G^3 curves and the B-spline curves are very similar, but the curvature of the G^3 curves is smoother than that of cubic B-spline curves 4.5. The knot intervals of all the examples are given as $d_i = l_i + l_{i+1} + l_{i+2}$, $i = 1, 2, \cdots, n-2$, where $l_j = |\mathbf{P}_{j-1}\mathbf{P}_j|$ is the length of polygon edge. In the example with end condition, we set $d_{-1} = d_0 = d_{n-1} = d_n = 0$ and in the other example, we set $d_{-1} = d_0 = d_1, d_n = d_{n-1} = d_{n-2}$.

Example 4.1. *Let* $P_0 = (241, 141), P_1 = (315, 101), P_2 = (364, 251), P_3 = (578, 249), P_4 = (629, 95), P_5 = (758, 82), P_6 = (833, 140)$. *The corresponding B-spline curve is shown in Figure* 4.1b. *We can clearly see that the curvature has some junctions. By using our new construction, after only three iterations, we can get the solution to be* $\overline{\Lambda} = \{\frac{1}{3}, 0.273429, 0.30181, 0.311446, 0.251477, \frac{1}{3}\}$.

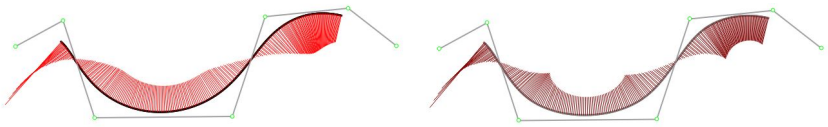

(a) The G^3 spline curve and the curvature comb (b) The cubic B-spline curve and the curvature comb

Fig. 4.1. Curvature combs of the two spline curves for the control polygon in Example 4.1.

Example 4.2. *Let* $P_0 = (408, 239), P_1 = (296, 308), P_2 = (155, 192), P_3 = (229, 48), P_4 = (420, 48), P_5 = (523, 184), P_6 = (693, 43), P_7 = (827, 112), P_8 = (796, 185)$. *After nine iterations, we get the solution to be* $\overline{\Lambda} = \{\frac{1}{3}, 0.243793, 0.389213, 0.268012, 0.266559, 0.301462, 0.243636, \frac{1}{3}\}$. *The curve and curvature information for both construction are shown in the Figure 4.2.*

Example 4.3. *The control points of the Example 3 in the figure 4.3 are* $P_0 = (219, 414)$, $P_1 = (79, 287)$, $P_2 = (98, 149)$, $P_3 = (269, 34)$, $P_4 = (446, 94)$, $P_5 = (483, 233)$, $P_6 = (465, 352)$, $P_7 = (366, 413)$ *with Bézier end condition. After optimization, we get* $\overline{\Lambda} = \{0, 0.619972, 0.300474, 0.342834, 0.290912, 0.66966, 0\}$.

Example 4.4. *The control points of this example are* $P_0 = (157, 156)$, $P_1 = (248, 118)$, $P_2 = (326, 171)$, $P_3 = (431, 119)$, $P_4 = (535, 201)$, $P_5 = (640, 123)$, $P_6 = (729, 170)$, $P_7 = (860, 123)$. *Then we solve the* $\overline{\Lambda} = \{0, 0.39748, 0.140545, 0.362066, 0.167863, 0.405231, 0\}$.

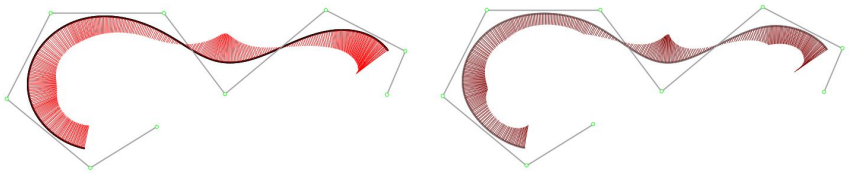

(a) The G^3 spline curve and curvature comb (b) The cubic B-spline curve and curvature comb

Fig. 4.2. Curvature combs of the spline curves for the control polygon in Example 4.2.

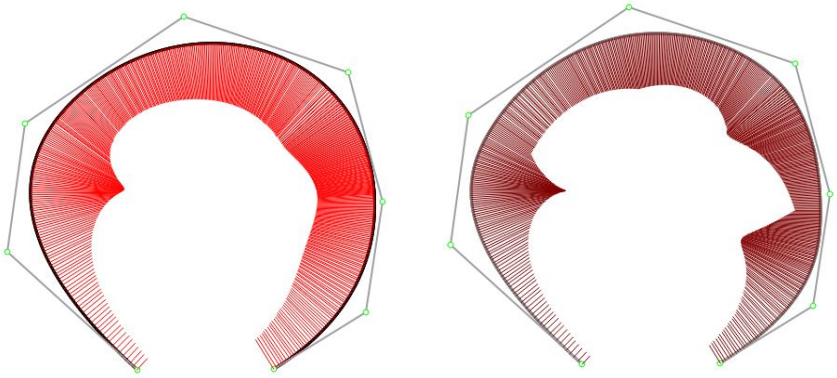

(a) The G^3 spline curve and curvature comb (b) The cubic B-spline curve and curvature comb

Fig. 4.3. Curvature combs of the two spline curves constructed from the control polygon in Example 4.3.

5. Conclusions and discussion

We have presented a method to construct a G^3 cubic spline curve with any given control polygon formed by a set of ordered points $\mathbf{P}_0, \mathbf{P}_1, \cdots, \mathbf{P}_n$ that satisfy $\Delta P_i \times \Delta P_{i+1} \neq 0$, $i = 0, 1, \cdots, n-1$. The constructing procedure involves to solve a non-linear system. Although we only prove that the solutions of the non-linear system exist under some constraints on the control polygon, but our numerical experiment show that the solution always exists. The curvature combs and curvature plots of G^3 cubic spline curve are smoother than C^2 spline curve because the curvature for the G^3 spline curve is C^1 continuous.

We only consider the construction for the open curve. The construction can be generalized to close curves. Actually, if the spline curve is a close curve, then the spline curve can be extracted into n Bézier segments. In this case, for each junction point $\mathbf{B}_{3i} (i = 0, 1, \cdots, n-1)$, we have n G^3 constraints which can be formalized into the similar non-linear equations with n unknowns. And we can solve the system in the same framework. However, we cannot prove the existence of the solution for the close curves. Example 5.1 gives a close curve where the G^3

(a) The G^3 spline curve and curvature comb (b) The cubic B-spline curve and curvature comb

Fig. 4.4. Curvature combs of the two spline curves constructed from the control polygon in Example 4.4.

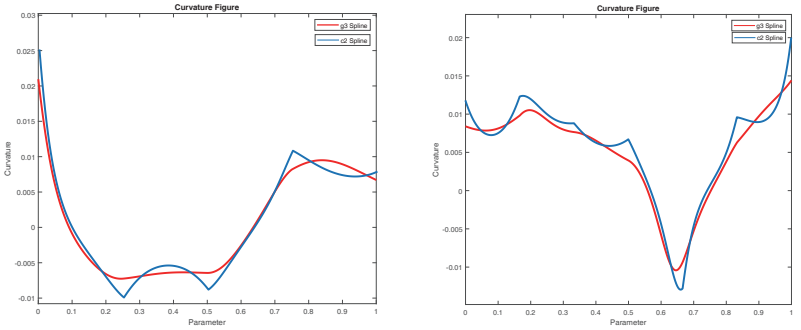

Curvature of example 4.1 Curvature of example 4.2

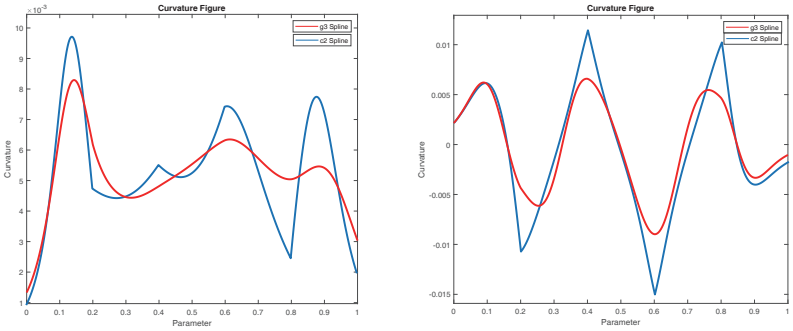

Curvature of example 4.3 Curvature of example 4.4

Fig. 4.5. The curvature plots for the four examples.

spline curve provides smoother curvature plots and curvature comb, see Figure 5.1.

Example 5.1. *Given a close control polygon with control points* $P_0 = (126, 446)$, $P_1 = (88, 257)$, $P_2 = (199, 64)$, $P_3 = (482, 103)$, $P_4 = (582, 265)$, $P_5 = (502, 468)$, $P_6 = (280, 524)$,, *we can solve the* $\overline{\Lambda} = \{0.301067, 0.372913, 0.268934, 0.394516, 0.278922, 0.341441, 0.321163\}$.

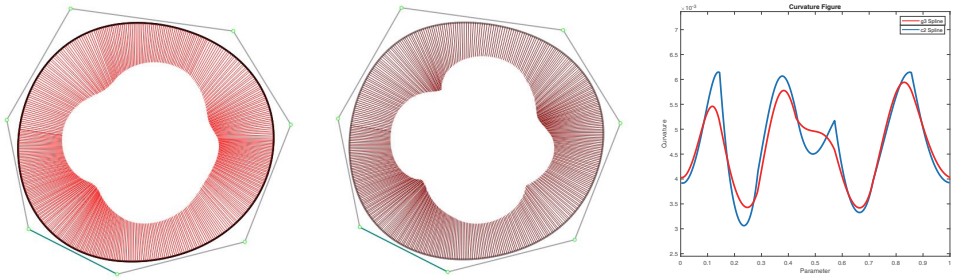

(a) The G^3 spline curve and curvature comb (b) The cubic B-spline curve and curvature comb (c) curvature plots

Fig. 5.1. Curvature combs and curvature plots of a close curve.

There are some problems worthy of further investigation. First, the constructing procedure for constructing G^3 cubic spline lacks locality. Once a new control point is added or a old control point is modified, the solution of the system 3.6 should be updated. Although the system can be solved in the realtime when the control points less than 50, but how to construct and modify

the spline locally is the most important problem to be considered. Second, theorem 3.1 cannot handle arbitrary situation. An improved proof of the existence will be left as a future work. Finally, how to generalize the approach to handle close curves and space curves is also a very interesting future problem.

Acknowledgments. The authors were supported by the NSF of China (No.61872328), NKBR-PC (2011CB302400), SRF for ROCS SE, and the Youth Innovation Promotion Association CAS.

References

[1] R. Barnhill and R. F. Riesenfeld, *Computer Aided Geometric Design*, Academic Press, 1974.
[2] L. Piegl and W. Tiller, *The NURBS Book*, Springer-Verlag, 1996.
[3] C. de Boor, *A Practical Guide to Splines*, Springer-Verlag, 1978.
[4] L. Schumaker, *Spline Functions: Basic Theory*, Addison-Wiley, 1981.
[5] C. de Boor, On calculating with B-splines, *Approx. Theory*, **6**:1(1972), 50-62.
[6] M. Cox, The numerical evaluation of B-splines, *Inst. Maths, Applies*, **10**:2(1972), 134-149.
[7] W. J. Gordon and R. F. Riesenfeld, B-spline curves and surfaces, *Computer Aided Geometric Design* **23**:91(1974), 95-126.
[8] B. A. Barsky, *The Beta-spline: a local representation based on shape parameters and fundamental geometric measures*, PhD thesis, University of Utah, 1981.
[9] B. A. Barsky, *Computer Graphics and Geometrie Modeling Using Beta-splines*, Springer-Verlag, 1988.
[10] T. N. Goodman, Properties of β-Splines, *Journal of Approximation Theory*, **44**:2(1985), 132-153.
[11] N. A. Hadi, A. Ibrahim, F. Yahya and J. Md Ali, A Comparative Study on Cubic Bezier and Beta-Spline Curves, *Malaysian Journal of Industrial and Applied Mathematics*, **29**:1(2013), 55-64.
[12] J. Manning, Continuity conditions for spline curves, *The Computer Journal*, **17**:2(1974), 181-186.
[13] G. M. Nielson, Some piecewise polynomial alternatives to splines under tension, *Computer Aided Geometric Design*, **23**:91(1974), 209-235.
[14] B. A. Barsky and T. DeRose, Geometric continuity of parametric curves, *IEEE Computer Graphics and Applications*, **9**:6(1989), 60-69.
[15] W. Böhm, On the definition of geometric continuity, *Comput. Aided. Des.*, **20**:7(1988), 370-372.
[16] R.T. Farouki and T. Sakkalis, Pythagorean hodographs, *IBM J. Res. Develop.*, **34**(1990), 736-752.
[17] J. Kosinka and M. Lávička, Pythagorean Hodograph curves: A survey of recent advances, *Journal for Geometry and Graphics*, **18**:1(2014), 23-43.
[18] R. Farouki, *Pythagorean-Hodograph curves*, Springer-Verlagr, 2008.
[19] C. Blanc and C. Schlick, X-splines: a spline model designed for the end-user, *Proceedings of SIGGRAPH 95*, 1995, pp. 377-386.
[20] D. J. Hartley and C. J. Judd, Parametrization of Bézier type B-spline curves and surface, *Computer-Aided Design*, **10**:2(1978), 130-134.
[21] G. Farin, Visually C^2 cubic splines, *Computer-Aided Design*, **14**:3(1982), 137-139.
[22] W. Böhm, Curvature continuous curves and surfaces, *Computer Aider Geometric Dsign*, **18**:2(1986), 105-106.
[23] I. J. Schoenberg, Spline functions, convex curves and mechanical quadrature, *Bull. Amer. Math. Soc.* **64**:6(1958), 352-357.
[24] L. Ramshaw, Blossoming: a connect-the-dots approach to splines, *Digital Systems Research*, 1987.
[25] L. Ramshaw, Béziers and B-splines as multiaffine maps, *Theoretical Foundations of Computer Graphics and CAD*, **40**(1989), 757-776.
[26] L. Ramshaw. Blossoms are polar forms. *Computer Aided Geometric Design*, **6**:4(1989), 323-358.

[27] T. W. Sederberg, J. Zheng, D. Sewell, and M. Sabin, Non-uniform recursive subdivision surfaces, *Proceedings of SIGGRAPH 98*, 1998, pp. 387-394.

[28] W. Böhm, Generating the Bézier points of B-spline curves and surfaces, *Computer-Aided Design*, **13**:6(1981), 365-366.

[29] G. Farin, *Curves and Surfaces for Computer Aided Geometric Design*, Morgan-Kaufmann, 2001.

[30] G. Farin, Curvature combs and curvature plots, *Computer-Aided Design*, **80**(2016), 6-8.

[31] G. Farin and N. Sapidis, Curvature and the fairness of curves and surfaces, *IEEE Comput Graph Appl*, **9**:2(1989), 52-57.

[32] H. Kang and X. Li, A New Method to Design Cubic Pythagorean-Hodograph Spline Curves with Control Polygon, *Communications in Mathematics and Statistics*, 2018.

[33] Z. Yan, S. Schiller, G. Wilensky, N. Carr and S. Schaefer, κ-curves: interpolation at local maximum curvature, *ACM Transactions on Graphics*, **36**:4(2017), 129.

[34] S. Robert, Interpolation with piecewise quadratic visually C^2 Bézier polynomials, *Computer Aided Geometric Design*, **6**:3(1989), 219-233.

[35] Y. Y. Feng and J. Kozak, On G^2 continuous interpolatory composite quadratic Bézier curves, *Journal of Computational and Applied Mathematics*, **72**:1(1996), 141-159.

[36] K.T. MiuraDai, D. Shibuya, R.U Gobithaasan and S. Usuki, Designing Log-aesthetic splines with G^2 continuity, *Computer-Aided Design and Applications*, **10**:6(2013), 1021-1032.